Available online at www.sciencedirect.com
SCIENCE DIRECT®
PHYSICS LETTERS B
ELSEVIER
Physics Letters B 567 (2003) 153–158
www.elsevier.com/locate/npe

First measurement and shell model interpretation of the g factor of the 2_1^+ state in self-conjugate radioactive ^{44}Ti

S. Schielke [a], K.-H. Speidel [a], O. Kenn [a], J. Leske [a], N. Gemein [a], M. Offer [a], Y.Y. Sharon [b], L. Zamick [b], J. Gerber [c], P. Maier-Komor [d]

[a] *Helmholtz-Institut für Strahlen- und Kernphysik, Universität Bonn, D-53115 Bonn, Germany*
[b] *Department of Physics & Astronomy, Rutgers University, New Brunswick, NJ 08903, USA*
[c] *Institut de Recherches Subatomiques, F-67037 Strasbourg, France*
[d] *Physik-Department, Technische Universität München, James-Franck-Str., D-85748 Garching, Germany*

Received 14 March 2003; received in revised form 17 June 2003; accepted 18 June 2003

Editor: V. Metag

Abstract

The g factor of the 2_1^+ state in radioactive ^{44}Ti has been measured for the first time with the technique of α transfer to ^{40}Ca beams in inverse kinematics in combination with transient magnetic fields, yielding the value, $g(2_1^+) = +0.52(15)$. In addition, the lifetimes of the 2_1^+, $\tau = 3.97(28)$ ps, and the 4_1^+ states, $\tau = 0.65(6)$ ps, were redetermined with higher precision using the Doppler shift attenuation method. The deduced B(E2)'s and the g factor were well explained by a full fp shell model calculation using the FPD6 effective NN interaction. The g factor can also be accounted for by a simple rotational model ($g = Z/A$). However, if one also considers the B(E2)'s and the $E(4_1^+)/E(2_1^+)$ ratios, then an imperfect vibrator picture gives better agreement with the data.

PACS: 21.10.Ky; 25.70.Hi; 27.40.+z

Keywords: g factor; ^{44}Ti, α-transfer reaction; ^{40}Ca beam; Inverse kinematics; Transient field

1. Introduction

The particular interest in $N = Z$ nuclei lies in the feature that both protons and neutrons occupy the same orbitals; hence isospin symmetry as well as neutron–proton pair correlations are the dominant features of the nuclear structure [1,2]. ^{44}Ti with $N = Z = 22$ is such a nucleus, with two valence protons and two valence neutrons in the $1f_{7/2}$ shell outside the doubly-magic ^{40}Ca ($N = Z = 20$) core.

The lowest 2_1^+ state in ^{44}Ti, like its 0_1^+ ground state, has isospin $T = 0$. Hence in measurements of the static magnetic and quadrupole moments of this excited state, as well as of the $B(\mathrm{E2}; 0_1^+ \to 2_1^+)$, we are picking out the isoscalar values. Up to now one could obtain a handle on, say, isoscalar g factors only by studying the ground state magnetic moments of $odd - A$ mirror nuclei. It was found in such studies [3] that the deviation from the Schmidt value is much smaller for isoscalar moments than for isovector moments.

E-mail address: speidel@iskp.uni-bonn.de (K.-H. Speidel).

0370-2693
doi:10.1016/j.physletb.2003.06.027

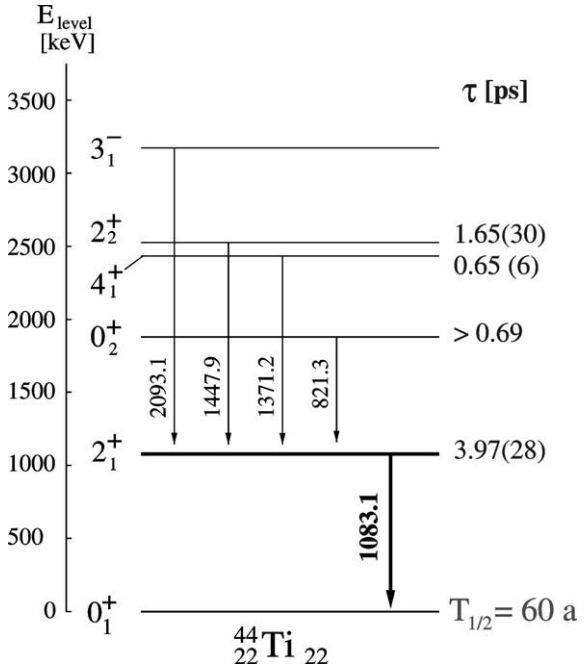

Fig. 1. Level scheme with relevant γ transitions. The lifetimes of the 2_1^+, 4_1^+ and 2_2^+ states are results of the present work (see text).

It is a well-known fact that magnetic moments and lifetimes of nuclear states are sensitive to the detailed composition of the nuclear wave functions. Since the spin g factors of protons and neutrons are different in sign and magnitude ($g_s^p = +5.586$, $g_s^n = -3.826$), such measurements enable one to determine the relative proton or neutron contributions in the nuclear state in question. This unique feature of magnetic moments and lifetimes has been used in many nuclei for testing nuclear model predictions [4], and it was shown that experimental g factor data need in general to be of few-percent precision to distinguish between the predictions of different models. For measuring magnetic moments of levels with *ps* lifetimes, where magnetic fields of *kilo* Tesla strengths are required, transient magnetic fields (TF) constitute at present the sole available experimental technique. As the field strength increases with ion velocity, the nuclear states to be studied should be populated in reactions for which the resulting nuclei emerge with high kinetic energies [4]. This condition is well satisfied by the technique of projectile Coulomb excitation in inverse kinematics: the nuclei of interest are fast projectiles (generally provided by an accelerator) which collide with light target nuclei, resulting in strong kinematic focussing and high ion velocities in the forward direction. As a consequence, highly efficient detection of target nuclei and coincident de-excitation γ rays of the projectiles is achieved. In particular, this technique was applied in recent measurements of g factors of the 2_1^+ and 4_1^+ states for the stable titanium nuclei ^{46,48,50}Ti, utilizing these isotopes as beams and carbon as a target [5–7]. The g factor trends observed were rather well explained within the framework of large-scale shell model calculations using an fp shell model space and a modified Kuo–Brown effective interaction. Inadequacies in the numerical agreement between the calculated and experimental results have been attributed to possible ^{40}Ca core excitations which were excluded for computational reasons.

In the present case of ^{44}Ti, projectile excitation would require a radioactive beam, a general approach which is presently being pursued in several laboratories. Due to the unavailability of such a beam an alternative technique was applied, which incorporates the merits of the inverse kinematics, as mentioned above, but is based on a particle-transfer reaction to stable beam nuclei. In several former measurements with projectile Coulomb excitation using carbon targets, α transfer was found to be a particularly strong reaction channel and has therefore been applied to g factor experiments. In this way $g(2_1^+)$ values were measured for radioactive ^{62}Zn obtained in α transfer to a ^{58}Ni beam [8] and also for ^{54}Cr using a ^{50}Ti beam [9]. In both cases, the 2_1^+ states were predominantly populated. This state selectivity is characteristic for the transfer mechanism and is distinctly different from that of a fusion/evaporation reaction in which high energy states are populated, feeding the low-lying states via cascade transitions. The reduced feeding in the case of α transfer ensures a clean measurement of the precession, as it is almost exclusively associated with that of the 2_1^+ state itself.

2. Experimental details

In the current experiment, a beam of isotopically pure ^{40}Ca was accelerated to an energy of 95 MeV at the Cologne tandem accelerator provid-

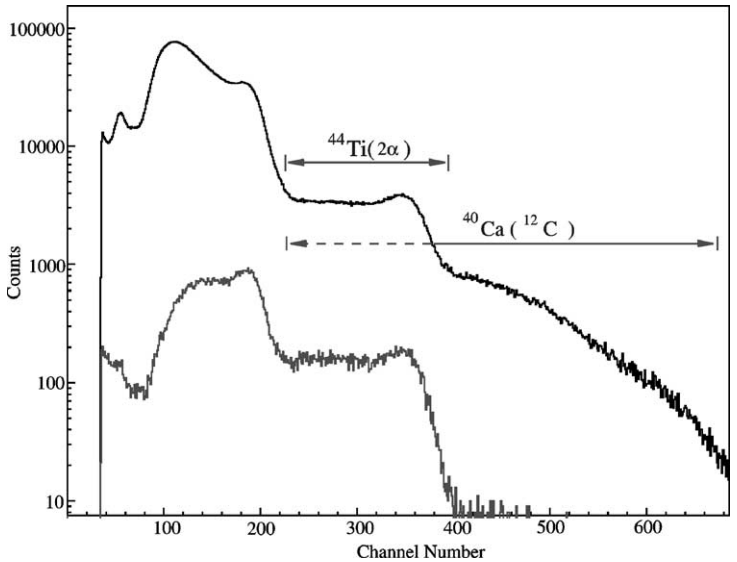

Fig. 2. Particle spectrum observed in coincidence with all γ-rays (upper spectrum). The lower spectrum refers to a gate on the $^{44}\mathrm{Ti}(2_1^+ \rightarrow 0_1^+)$ γ transition only. Gates for γ-coincidence spectra are indicated for ^{44}Ti and ^{40}Ca, respectively (see text).

ing intensities of (2–3) pnA on a multilayered target. The target consisted of 0.45 mg/cm^2 $^{\mathrm{nat}}$C, deposited on 3.82 mg/cm^2 Gd, which was evaporated on a 1.0 mg/cm^2 Ta foil, backed by a 3.48 mg/cm^2 Cu layer. For the Gd evaporation, the tantalum substrate was kept at a temperature of 800 K to ensure good magnetic properties of gadolinium [11]. Besides Coulomb excitation of the ^{40}Ca projectiles in collisions with carbon nuclei, essentially to the first 3^- state at 3.736 MeV, strong α transfer occurred in the $^{12}\mathrm{C}(^{40}\mathrm{Ca}, ^{8}\mathrm{Be})^{44}\mathrm{Ti}$, whereby the $^{44}\mathrm{Ti}(2_1^+)$ state of interest was predominantly populated; weak excitations of the 4_1^+, 2_2^+ and 3_1^- states were also observed (see Fig. 3). The relevant level scheme of ^{44}Ti is shown in Fig. 1. The residual nuclei ^{40}Ca and ^{44}Ti from Coulomb excitation and α transfer, respectively, both move through the Gd layer at high velocities in the direction of the primary ^{40}Ca beam for spin precessions. These nuclei came to rest in the hyperfine interaction-free environment of the copper backing.

The de-excitation γ rays were measured in coincidence with forward scattered ions, either carbon ions or 2α particles from the decay of ^{8}Be. Both types of ions pass through the target layers and an additional Ta foil and are detected in a 100 μm Si counter placed at 0° relative to the beam axis. The Ta foil between target and particle detector served as beam stopper. The Si detector, subtending an angle of $\pm 30°$, was operated with a low bias of 3–5 V (instead of the nominal 40 V). This enabled a better separation of the 2α particles associated with ^{44}Ti (and other light charged particles such as protons) from the heavier carbon ions due to their different stopping behaviour in a thus reduced depletion layer of the Si detector. This separation procedure was already successfully applied in several earlier measurements (see, e.g., [6] and Fig. 2).

Four 12.7 cm × 12.7 cm NaI(Tl) scintillators and a Ge detector with a relative efficiency of 40% were used for γ detection. Coincident particle and γ spectra are shown in Figs. 2 and 3. The Ge detector placed at 0°, served as a monitor for contaminant lines in the energy region of interest and to measure nuclear lifetimes via the Doppler Shift Attenuation Method (DSAM).

Detailed $(2\alpha{-}\gamma)$-angular correlations $W(\Theta_\gamma)$ have been measured for determining the slope $S = [1/W(\Theta_\gamma)\,\mathrm{d}W(\Theta_\gamma)/\mathrm{d}\Theta_\gamma]$ in the rest frame of the γ-emitting nuclei at angles $\Theta_\gamma = 65°$ where the experimental sensitivity to the spin precessions is optimal. Precession angles, Φ^{exp}, were determined in the normal way via counting rate ratios R for 'up' and

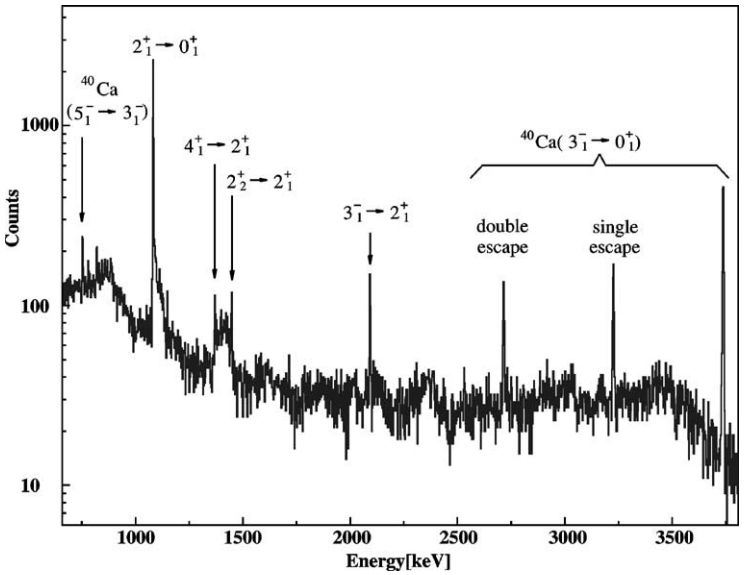

Fig. 3. γ-coincidence spectrum observed with the 0° Ge detector with the particle gate on ^{44}Ti events (see Fig. 2).

'down' directions of the external field with detector pairs placed symmetrically to the beam direction. The precession angles were derived [4] as:

$$\Phi^{\exp} = \frac{1}{S}\frac{\sqrt{R}-1}{\sqrt{R}+1} = g\frac{\mu_N}{\hbar}\int_{t_{\text{in}}}^{t_{\text{out}}} B_{\text{TF}}\big(v_{\text{ion}}(t)\big)e^{-t/\tau}\,dt, \tag{1}$$

where g is the g factor of the 2_1^+ state and B_{TF} the transient field acting for the time interval $(t_{\text{out}} - t_{\text{in}})$ that the ions spend in the gadolinium layer; the exponential accounts for the decay of the 2_1^+ state with lifetime τ.

The lifetimes of the 2_1^+, 4_1^+ and 2_2^+ states were redetermined from measured lineshapes of the three γ lines using the DSAM technique with the 0° Ge detector. The high ion velocities result in high sensitivity for the lifetimes in the ps range. The Doppler-broadenend lineshapes were fitted for the reaction kinematics applying stopping powers [12] to Monte Carlo simulations including the second order Doppler effect as well as the finite size and energy resolution of the Ge detector. Feeding from higher states was also taken into account. The computer code LINESHAPE [13] was used in the analysis.

Table 1
Summary of the slope of the measured angular correlation, the experimental precession angle and the deduced g factor and lifetimes. Comparison to earlier lifetime data [10] is shown

E_x (MeV)	τ (ps)		$\lvert S(65°)\rvert$	$\Phi_{\exp}$ (mrad)	$g(2_1^+)$
	[10]	present			
2_1^+: 1.083	4.5(12)	3.97(28)	0.423(55)	17.6(4.9)	+0.52(15)
4_1^+: 2.454	0.60(10)	0.65(6)	–	–	–
2_2^+: 2.531	1.40(20)	1.65(30)	–	–	–

3. Results and discussion

The g factor of the 2_1^+ state was derived from the experimental precession angle $\Phi^{\exp}$ by determining the effective TF on the basis of the linear parametrization [4]:

$$B_{\text{TF}}(v_{\text{ion}}) = G_{\text{beam}} \cdot B_{\text{lin}} \tag{2}$$

with

$$B_{\text{lin}} = a(\text{Gd}) \cdot Z_{\text{ion}} \cdot (v_{\text{ion}}/v_0), \tag{3}$$

where the strength parameter $a(\text{Gd}) = 17(1)$ Tesla, $v_0 = e^2/\hbar$, and $G_{\text{beam}} = 0.90(5)$ is the attenuation factor of the TF strength induced by the calcium beam used [4].

Table 2
Experimental data in comparison with results from fp shell model calculations using the effective interactions KB3 and FPD6

Quantity	Experimental	KB3		FPD6	
		$(f_{7/2})^4$	full fp shell	$(f_{7/2})^4$	full fp shell
$E(2_1^+)$ (MeV)	1.083	0.570	1.393	0.943	1.296
$E(4_1^+)$ (MeV)	2.454	1.576	2.549	1.941	2.495
$g(2_1^+)$	+0.52(15)	+0.554	+0.532	+0.554	+0.514
$Q(2_1^+)$ (eb)	–	+0.147	−0.096	+0.135	−0.218
$B(\mathrm{E2}; 0_1^+ \to 2_1^+)$ ($e^2\mathrm{b}^2$)	0.069(5)	0.032	0.058	0.031	0.070
$B(\mathrm{E2}; 2_1^+ \to 4_1^+)$ ($e^2\mathrm{b}^2$)	0.047(4)	0.015	0.027	0.014	0.034
$B(\mathrm{E2}; 0_1^+ \to 2_2^+)$ ($e^2\mathrm{b}^2$)	0.0006(1)	0.0005	0.0022	0.0002	0.00002
$B(\mathrm{E2}; 2_1^+ \to 2_2^+)$ ($e^2\mathrm{b}^2$)	0.0057(10)	0.0008	0.0151	0.0017	0.0060

The precession and lifetime data with the deduced g factor for ^{44}Ti are summarized in Table 1. The new lifetime values are in good agreement with the earlier data but are of higher or comparable precision.

The $g(2_1^+)$ factor and the $B(\mathrm{E2})$ values deduced from the lifetimes of the 2_1^+, 4_1^+ and 2_2^+ states have been interpreted within the framework of the nuclear shell model. The calculations were carried out using the shell model code OXBASH [14] and both the KB3 [15] and the FPD6 [16] effective NN-interactions. In these calculations ^{44}Ti is considered to consist of an inert ^{40}Ca core with four valence nucleons, two protons and two neutrons. The results are compared with the experimental data in Table 2. We also calculated a value for the unmeasured quadrupole moment of the 2_1^+ state, that can be compared to corresponding measured values for neighbouring nuclei ranging from $-0.14(7)$ eb for ^{44}Ca to $-0.21(6)$ eb for ^{46}Ti [17].

The simplest approach is an $(f_{7/2})^4$ configuration which, however, is obviously inadequate as evident from the table. With that configuration both interactions usually underestimate the $B(\mathrm{E2})$'s by more than a factor of two (suggesting that not enough collectivity is provided), and predict a positive quadrupole moment $Q(2_1^+)$. The only quantity that is rather well reproduced, for reasons to be explained later, is the $g(2_1^+)$, where both interactions yield an identical value of $g(2_1^+) = +0.554$.

The situation is greatly improved by full fp shell calculations, in which the four valence nucleons can occupy the $1f_{7/2}$, $2p_{3/2}$, $1f_{5/2}$ and $2p_{1/2}$ orbitals. As shown in Table 2, the calculations with the FPD6 interaction account very well for the experimental data without requiring any admixture, into the 2_1^+ wave function, of particle-hole excitations from the ^{40}Ca core. Similarly, almost as good results were obtained with the KB3 interaction. The FPD6 full fp shell calculation, however, underestimates the extremely small $B(\mathrm{E2}; 0_1^+ \to 2_2^+)$ by an order of magnitude, whereas the $B(\mathrm{E2}; 2_1^+ \to 2_2^+)$ is very well reproduced. On the other hand, in a pure vibrational model the $(2_2^+ \to 0_1^+)$ transition would be a forbidden two-phonon transition implying a vanishing $B(\mathrm{E2})$.

It is worthwhile attempting to understand why the simple $(f_{7/2})^4$ configuration accounts as well for the $g(2_1^+)$ as the full fp shell calculations. To this end, the individual components of the 2_1^+ wave function obtained in the full fp calculations have been examined. In the FPD6 calculation the major component intensities are $(f_{7/2})^4$ (26%), $(f_{7/2})^3(p_{3/2})^1$ (24%) and $(f_{7/2})^2(p_{3/2})^2$ (10%); in the KB3 calculations the same components have intensities of 54%, 15% and 7%, respectively. Evidently the $p_{3/2}$ orbital plays a more important role here than do the $f_{5/2}$ and the $p_{1/2}$ orbitals, a feature which was also found for ^{44}Ca [18, 19]. One then finds that the other two main configurations in the 2_1^+ wave function (see above) have $g(2_1^+)$ values close to that for the $(f_{7/2})^4$ for which $g(2_1^+) = +0.554$; for both interactions, $g(2_1^+) = +0.519$ for $(f_{7/2})^3(p_{3/2})^1$ and $+0.575$ for $(f_{7/2})^2(p_{3/2})^2$. Since all of these values are very close to the experimental value a distinction between the two interactions would require a precision of the experimental value on a 1% level, which, however, cannot be achieved with the present technique. On the other hand, the most important perturbing configuration, $(f_{7/2})^3(p_{3/2})^1$, has a very different $Q(2_1^+)$ value than the $(f_{7/2})^4$. With FPD6 one obtains: $Q(2_1^+) = +0.135$ eb for $(f_{7/2})^4$

and -0.150 eb for $(f_{7/2})^3(p_{3/2})^1$; with KB3 similar values are obtained. Thus the $(f_{7/2})^3(p_{3/2})^1$ configuration plays an important role in the full fp shell calculations in giving rise to the expected negative sign of $Q(2_1^+)$.

The $g(2_1^+)$ can be calculated analytically for the $(f_{7/2})^4$ configuration using an expression (Eq. (28) in Ref. [20]) derived by McCullen, Bayman and Zamick for configurations of nucleons in a single j shell. For $N = Z$ nuclei (e.g., ^{44}Ti) this expression simplifies in the $f_{7/2}$ shell to

$$g = \left[\frac{g_p + g_n}{2}\right]_{\text{Schmidt}} = \frac{1.655 + (-0.547)}{2} = +0.554 \quad (4)$$

independent of the details of the wave function.

It is interesting to note that simple collective model formulae also explain well some of the properties of the 2_1^+ state in ^{44}Ti. The g factor of the collective model [21], $g = Z/A = +0.5$, is in good agreement with the experimental result. Furthermore, from the experimental $B(\text{E2}; 0_1^+ \to 2_1^+) = 0.069\, e^2\text{b}^2$ one derives an intrinsic quadrupole moment $Q_0 = [16\pi/5\, B(\text{E2})/e^2]^{1/2}$ and finally $Q(2_1^+) = -2/7\, Q_0 = |-0.235|$ eb close in magnitude to the result of the full fp shell calculation with FPD6 (Table 2). Moreover, from the $B(\text{E2})$ value a deformation $\beta = 0.28$ can be deduced that is consistent with the values of 0.25 for ^{44}Ca and 0.32 for ^{42}Ti and ^{46}Ti [22].

The observed value of the ratio $B(\text{E2}; 2_1^+ \to 4_1^+)/B(\text{E2}; 0_1^+ \to 2_1^+)$ is 0.68. All four shell model calculations (see Table 2) predict this ratio to be between 0.45 and 0.49. The collective predictions for this ratio are 0.51 in the rotational model but 0.72 in the vibrational model, closer to what is observed. The ratio of the experimental excitation energies $E(4_1^+)/E(2_1^+)$ is 2.27, again quite close to the pure vibrational value of 2.

In summary, we note that the $g(2_1^+)$ measurement is accounted for by all four shell model calculations in Table 2 and the Z/A collective value. However, only the FPD6 full fp shell calculations fully account for our newly measured, more precise, $B(\text{E2}; 0_1^+ \to 2_1^+)$ value of $0.069(5)\, e^2\text{b}^2$ as well as the $B(\text{E2}; 2_1^+ \to 2_2^+)$ of $0.0057(10)\, e^2\text{b}^2$.

Acknowledgements

The authors are grateful to the operators of the tandem accelerator. They acknowledge the support of the BMBF, the Deutsche Forschungsgemeinschaft, the US Department of Energy under Grant DE-FG02-95ER-40940, and a Stockton College Sabbatical Grant to Y.Y.S.

References

[1] A.L. Goodman, Phys. Rev. C 58 (1998) R3051.
[2] T. Otsuka, et al., Nucl. Phys. 47 (2001) 319.
[3] L. Zamick, Phys. Rev. C 15 (1977) 824.
[4] K.-H. Speidel, O. Kenn, F. Nowacki, Prog. Part. Nucl. Phys. 49 (2002) 91.
[5] R. Ernst, et al., Phys. Rev. Lett. 84 (2000) 416.
[6] R. Ernst, et al., Phys. Rev. C 62 (2000) 024305.
[7] K.-H. Speidel, et al., Phys. Rev. C 62 (2000) 031301(R).
[8] O. Kenn, et al., Phys. Rev. C 65 (2002) 034308.
[9] S. Wagner, et al., Phys. Rev. C 64 (2001) 034320.
[10] J.A. Cameron, B. Singh, Nucl. Data Sheets 88 (1999) 380.
[11] P. Maier-Komor, K.-H. Speidel, A. Stolarz, Nucl. Instrum. Methods Phys. Res. A 334 (1993) 191.
[12] F.J. Ziegler, J. Biersack, U. Littmark, in: The Stopping and Range of Ions in Solids, Vol. 1, Pergamon, Oxford, 1985.
[13] J.C. Wells, N.R. Johnson, computer code LINESHAPE, ORNL, 1994.
[14] A. Etchegoyen, W.D. Rae, N.S. Godwin, W.A. Richter, C.H. Zimmerman, B.A. Brown, W.E. Ormand, J.S. Winfield, computer code OXBASH, MSU-NSCL Report No. 524, 1985, unpublished.
[15] A. Poves, A. Zuker, Phys. Rep. 70 (1981) 235.
[16] W.A. Richter, M.G. Van der Merwe, R.E. Julies, B.A. Brown, Nucl. Phys. A 253 (1991) 325.
[17] P. Raghavan, At. Data Nucl. Data Tables 42 (1989) 189.
[18] S. Schielke, et al., submitted to Phys. Lett. B.
[19] M.J. Taylor, et al., Phys. Lett. B 559 (2003) 187.
[20] J.D. McCullen, B.F. Bayman, L. Zamick, Phys. Rev. 134 (1964) B515.
[21] A. Bohr, B.R. Mottelson, in: Nuclear Structure, Vol. 2, Benjamin, New York, 1975.
[22] S. Raman, C.W. Newsor Jr., P. Tikkanen, At. Data Nucl. Data Tables 78 (2001) 1.